Accepted Manuscript

Phytochemical constituents from Uncaria rhynchophylla in human carboxylesterase 2 inhibition: Kinetics and interaction mechanism merged with docking simulations

Ya-Li Wang , Pei-Pei Dong , Jia-Hao Liang , Ning Li , Cheng-Peng Sun , Xiang-Ge Tian , Xiao-Kui Huo , Bao-Jing Zhang , Xiao-Chi Ma , Chuan-Zhu Lv

PII: S0944-7113(18)30527-0
DOI: https://doi.org/10.1016/j.phymed.2018.10.006
Reference: PHYMED 52709

To appear in: *Phytomedicine*

Received date: 11 September 2018
Revised date: 27 September 2018
Accepted date: 9 October 2018

Please cite this article as: Ya-Li Wang , Pei-Pei Dong , Jia-Hao Liang , Ning Li , Cheng-Peng Sun , Xiang-Ge Tian , Xiao-Kui Huo , Bao-Jing Zhang , Xiao-Chi Ma , Chuan-Zhu Lv , Phytochemical constituents from Uncaria rhynchophylla in human carboxylesterase 2 inhibition: Kinetics and interaction mechanism merged with docking simulations, *Phytomedicine* (2018), doi: https://doi.org/10.1016/j.phymed.2018.10.006

This is a PDF file of an unedited manuscript that has been accepted for publication. As a service to our customers we are providing this early version of the manuscript. The manuscript will undergo copyediting, typesetting, and review of the resulting proof before it is published in its final form. Please note that during the production process errors may be discovered which could affect the content, and all legal disclaimers that apply to the journal pertain.

ACCEPTED MANUSCRIPT

Phytochemical constituents from *Uncaria rhynchophylla in* human carboxylesterase 2 inhibition: Kinetics and interaction mechanism merged with docking simulations

Ya-Li Wang[a,b,+], Pei-Pei Dong[a,+], Jia-Hao Liang[a,+], Ning Li[b], Cheng-Peng Sun[a,*], Xiang-Ge Tian[a], Xiao-Kui Huo[a], Bao-Jing Zhang[a], Xiao-Chi Ma[a], Chuan-Zhu Lv[c,*]

[a] *College of Pharmacy, College (Institute) of Integrative Medicine, The National & Local Joint Engineering Research Center for Drug Development of Neurodegenerative Disease, Dalian Medical University, Dalian, China.*

[b] *Key Laboratory of Structure-Based Drug Design & Discovery, Ministry of Education, Department of Natural Products Chemistry, School of Traditional Chinese Materia Medica, Shenyang Pharmaceutical University, Shenyang, China*

[c] *Institute of Functional Materials and Molecular Imaging, College of Emergency and Trauma, Hainan Medical University, Haikou, China*

[+]*These authors contributed equally to this work.*

Corresponding authors at: College of Pharmacy, Dalian Medical University, Dalian, China. E-mail: suncp146@163.com (C.P. Sun); Hainan Medical University, Haikou, China. E-mail: lvchuanzhu677@126.com (C.Z. Lv).

ACCEPTED MANUSCRIPT

ABSTRACT:

Background: Carboxylesterases (CEs) belong to the serine hydrolase family, and are in charge of hydrolyzing chemicals with carboxylic acid ester and amide functional groups via Ser-His-Glu. *Uncaria rhynchophylla* (Miq.) Miq. ex Havil. is a famous traditional Chinese medicine used in managing hyperpyrexia, epilepsy, preeclampsia, and hypertension in China.

Hypothesis/purpose: To discover the potential natural human carboxylesterase 2 (hCE 2) inhibitors from *U. rhynchophylla*.

Methods: Compounds were obtained from the hooks of *U. rhynchophylla* by silica gel and preparative HPLC. Their structures were elucidated by using HRESIMS, 1D and 2D NMR spectra. Their inhibitory activeties and inhibition kinetics against hCE 2 were assayed by the fluorescent probe, and potential mechanisms were also investigated by molecular docking.

Results: Twenty-three compounds, including a new phenolic acid uncariarhyine A (**1**), eight known triterpenoids (**2**-**9**), and ten known aromatic derivatives (**10**, **13**-**16**, and **19**-**23**), were isolated from *U. rhynchophylla*. Compounds **1**-**5**, **7**, **9**, and **15** showed significant inhibitory activities against hCE 2 with IC_{50} values from 4.01 ± 0.61 μM to 18.60 ± 0.21 μM, and their inhibition kinetic analysis results revealed that compounds **1**, **5**, **9**, and **15** were non-competitive; compounds **3** and **4** were mixed-type, and compounds **2** and **7** were uncompetitive. Molecular docking studies indicated inhibition mechanisms of compounds **1**-**5**, **7**, **9**, and **15** against hCE 2.

Conclusion: Our present findings highlight potential natural hCE 2 inhibitors from *U. rhynchophylla.*

ACCEPTED MANUSCRIPT

Keywords: *Uncaria rhynchophylla*; Human carboxylesterase 2; Triterpenoid; Kinetics; Molecular docking

Abbreviations: CEs, carboxylesterases; hCE 1, human carboxylesterase 1; hCE 2, human carboxylesterase 2; HLM, Human liver microsome

Introduction

Carboxylesterases (CEs) belong to the serine hydrolase family (Bencharit et al., 2006; Satoh and Hosokawa, 1998; Soares da Silva et al., 2018; Zou et al., 2016), and are in charge of hydrolyzing chemicals with carboxylic acid ester and amide functional groups via Ser-His-Glu (Zhang et al., 2017). They widely distributed in mammalian tissues as critical phase I metabolizing enzymes, and regulate metabolism of ester compounds and detoxication of environmental toxins (Potter and Wadkins, 2006; Wheelock et al., 2008; Zou et al., 2016). Human carboxylesterases (hCE) are classified into two subtypes, human carboxylesterase 1 (hCE 1) and human carboxylesterase 2 (hCE 2) (Xin et al., 2018). hCE 1 is abundantly expressed in the liver, whereas hCE 2 is predominately expressed in the gastrointestinal tract (Xin et al., 2018; Zhang et al., 2017). The expression of hCE 2 in enterocytes may represent a defensive barrier for esterified drugs before the organism is exposed following ingestion (Ross and Crow, 2007). Thus, CEs is regarded as a crucial enzyme to regulate oral drugs containing ester groups in the first-pass effect (Zou et al., 2016), and development of new CEs inhibitors is extremely urgent (Binder et al., 2018;

ACCEPTED MANUSCRIPT

Hatfield et al., 2017; Zou et al., 2016).

Medicinal plants are important sources to search for new hCE 2 inhibitors (Xin et al., 2018; Zhang et al., 2017). The genus *Uncaria* belongs to the family Rubiaceae, which currently consists of 34 species and is widely distributed in the tropical regions, such as Southeast Asia, Africa, and South America (Ndagijimana et al., 2013; Zhang et al., 2015). As a famous traditional Chinese medicine (TCM), *U. rhynchophylla* (Miq.) Miq. ex Havil., known as "Gou-Teng" in Chinese, has been not only used to treat hyperpyrexia, epilepsy, preeclampsia, and hypertension, but also used in Japan, Malaysia, Singapore, Peru, Guayana, and Brazil (Geng et al., 2017; Li et al., 2017; Ndagijimana et al., 2013). Previous studies have revealed that alkaloids and triterpenoids are the major constituents of the genus *Uncaria* (Ndagijimana et al., 2013; Zhang et al., 2015), and some triterpenoids display significant inhibitory activities against hCE 2 (Zou et al., 2016). Therefore, as part of our continuous research on the discovery of natural hCE 2 inhibitors from TCM (Cang J et al., 2017; Huo et al., 2018; Wang et al., 2017; Yu et al., 2017), EtOH extracts of hooks of *U. rhynchophylla* were investigated which resulted in the isolation of a new compound **1** together with twenty-two known compounds **2-23**. All the isolated compounds were determined on the basis of 1D and 2D NMR, and HRESIMS analyses. We evaluated their hCE 2 inhibitory activities and enzyme kinetics *in vitro*. Structure-activity relationship of ursane-type triterpenoids was discussed. Molecular docking was used to investigate potential interactions between inhibitors and hCE 2.

Material and methods

General Experimental Procedures.

Perkin-Elmer 241 polarimeter was used to record optical rotations. UV spectra were recorded on a Shimadzu UV 2201 spectrophotometer. ECD spectra were recorded on a Bio-Logic Science MOS-450 spectrometer. Bruker AV-600 spectrometer was used in the NMR experiments. Chemical shift values were expressed in δ (ppm) using the peak signals of the solvent DMSO-d_6 (δ_H 2.50 and δ_C 39.5) as a reference, and coupling constants (J in Hz) were given in parentheses. HRESIMS data were acquired on an Agilent 6210 TOF mass spectrometer. Preparative HPLC was performed on an Elite P2300 instrument with an Elite UV2300 detector (Dalian, China) and a YMC C_{18} column (250 mm × 10 mm, 5 μm). All solvents were obtained from Tianjin Kemiou Chemical Reagent Company (Tianjing, China), MeOH for HPLC analysis was chromatographic grade (Merck, Darmstadt, Germany). Silica gel (200−300 mesh) was purchased from Qingdao Marine Chemical Factory (Qingdao, China). Some analogues of ursane-type triterpenoids, 24-*epi*-pinfaensic acid (**24**), 24-*epi*-pinfaesin (**25**), ursolazuroside 1 (**26**), tormentic acid (**27**), hyptatic acid B (**28**), and niga-ichigosode F1 (**29**) were previously separated from *Glycyrrhiza uralensis* Fisch. (Fig. 1) by authors, and their purities were more than 98% analyzed by HPLC. Human liver microsome (HLM) were purchased from Research Institute of Liver Diseases (Shanghai) Co., Ltd., China.

Plant Material.

Dried hooks of *U. rhynchophylla* were purchased in March 2017 from Beijing Tongrentang Co., Ltd., China, and identified by Prof. Jing-Ming Jia, Shenyang Pharmaceutical University. A voucher specimen (UR201704) has been deposited in

ACCEPTED MANUSCRIPT

the herbarium of the Department of Medicinal Chemistry, Dalian Medical University.

Extraction and Isolation.

Dried hooks of *U. rhynchophylla* (18 kg) were extracted with 95% EtOH (2 × 2 h × 180 L) and 75% EtOH (1 × 2 h × 180 L) to afford a residue after solvent removal *in vacuo*. The residue (2.1 kg) was suspended by H_2O (10 L) and extracted with CH_2Cl_2 (3 × 10 L) and *n*-BuOH (3 × 10 L), successively.

CH_2Cl_2 extracts (300 g) was subjected to silica gel column chromatography (CC) eluted with CH_2Cl_2-MeOH (100:1 to 1:1), yielding seven fractions C1-C7. Faction C4 (40 g) was separated by silica gel CC with a gradient of acetone in CH_2Cl_2 ranging from 1% to 100% to produce seven subfractions C41−C47. Subfraction C42 (12 g) was subjected to a silica gel column eluted with petroleum ether-acetone (100:1 to 1:1) to afford seven subfractions C421-C425. Separation of subfraction C421 (2 g) by ODS CC (MeOH-H_2O, 10% to 100%) and preparative HPLC (MeOH-H_2O, 45% to 85%) resulted in the isolation of compounds **1** (4 mg), **2** (134 mg), **4** (2 mg), **12** (3.7 mg), **13** (2 mg), and **16** (3.6 mg).

Subfraction C47 (2.8 g) was separated by silica gel CC eluted with petroleum ether-acetone (100:1 to 1:1) to afford seven subfractions C471-C477. Purification of subfraction C474 (0.5 g) through preparative HPLC (MeOH-H_2O, 60% to 75%) yielded compounds **10** (4.8 mg), **11** (7.3 mg), and **14** (2 mg). Fraction C5 (50 g) was purified by silica gel CC eluted with CH_2Cl_2-MeOH (100:1 to 1:1) to afford nine subfractions C51-C59. Subfraction C51 (30 g) was separated by a silica gel column eluted with petroleum ether-acetone (100:1 to 1:1), yielding five subfractions C511-C515. Compounds **3** (11.2 mg) and **17** (6.7 mg) were afforded from subfraction C511 (3 g) by preparative HPLC eluted with MeOH-H_2O (60%). Subfraction C58 (3.58 g) was separated by silica gel CC (CH_2Cl_2-acetone, 50:1 to 1:1) and preparative

HPLC (MeOH-H_2O, 90%) to afford compound **15** (9.2 mg).

n-BuOH extract (400 g) was purified by D101 resins and eluted with EtOH-H_2O (10% to 95%) to afford four fraction B1-B4. Fraction B3 (190 g) was separated through a silica gel column eluted with CH_2Cl_2-MeOH (100:1 to 1:1) to afford six subfractions B31-B36. Subfraction B31 (7.2 g) was subjected to a silica gel column eluted with petroleum ether-acetone (50:1 to 1:2) to afford three subfractions B311-B313. Separation of subfraction B31 (100 mg) by preparative HPLC (MeOH-H_2O, 75% to 100%) led to the isolation of compound **19** (3.6 mg). Subfraction B312 (500 mg) was purified by preparative HPLC (MeOH-H_2O, 60% to 90%), yielding compounds **5** (70.2 mg), **6** (67.1 mg), **7** (3.1 mg), **8** (4 mg), **9** (2 mg), **20** (5 mg), **21** (3.6 mg), **22** (3.6 mg), and **23** (3 mg).

Uncariarhyine A (**1**): amorphous powder; $[\alpha]_D^{20}$ − 101 (*c* 0.1, MeOH); UV (MeOH) λ_{max} (log ε) 211 (4.1) nm; ^{1}H (600 MHz, DMSO-d_6) and ^{13}C NMR (150 MHz, DMSO-d_6) data, see Table 1; HRESIMS *m/z* 483.3840 $[M + H]^+$ (calcd. for $C_{32}H_{51}O_3$, 483.3838).

hCE 2 inhibitory activity

hCE 2 inhibitory activities of compounds **1-29** were performed using our pervious method (Zhang et al., 2017). Compounds **1-29** were dissolved in DMSO and diluted to final concentrations from 0.1 μM to 200.0 μM. All compounds were hydrolyzed by HLM at 37 ℃ with the probe substrate 4-benzoyl-*N*-butyl-1,8-naphthalimide (MPN) in a 96-well plate, then the fluorescence signal was detected at 564 nm. The probe substrate groups (without evaluated compounds) were used as control. Loperamide was used as a control drug.

Inhibitory kinetic analysis

ACCEPTED MANUSCRIPT

ACCEPTED MANUSCRIPT

Kinetic analysis of hCE 2 enzyme for compounds **1-5**, **7**, **9**, and **15** was conducted by using the Lineweaver-Burk and Dixon analyses. The experiment was conducted at different MPN concentrations from 0.02 μM to 20 μM in the absence and presence of compounds **1-5**, **7**, **9**, and **15**.

Molecular docking

The homology structure of hCE 2 built using the Modeller (version 9) program as described before was used to probe the inhibition mechanism (Zhang et al., 2017). The 3D structure of each molecule was subjected to energy minimization with the default Tripos force field parameters, and the Gasteiger-Hückel charges were calculated. The bioactive binding conformations of compounds **1-5**, **7**, **9**, and **15** within hCE 2 were probed using Surflex-Dock, which were evaluated by an empirical function Chemscore (Ai et al., 2010).

Statistical analysis

The statistical analysis was performed with GraphPadPrism 7.0. The differences among the extracts were evaluated by one-way analysis of variance (ANOVA) followed by Dunnett's multiple comparison test ($p < 0.05$). All data are presented as means ± SD.

Results and discussion

Structural identification

Compound **1** was isolated as a white powder with the molecular formula of $C_{32}H_{50}O_3$ based on a quasi-molecular ion peak at *m/z* 483.3840 $[M + H]^+$ (calcd. for $C_{32}H_{51}O_3$, 483.3838) in the HRESIMS spectrum. The ^1H NMR data (Table 1) of **1**

displayed signals of six aromatic protons at δ_H 7.37 × 2 (2H, d, J = 2.4 Hz, H-3 and H-3′), 7.29 × 2 (2H, dd, J = 8.5, 2.4 Hz, H-5 and H-5′), and 7.08 × 2 (2H, d, J = 8.5 Hz, H-6 and H-6′), and signals of twelve methyl groups at δ_H 1.39 × 6 (18H, s, CH_3-8, CH_3-8′, CH_3-9, CH_3-9′, CH_3-10, and CH_3-10′) and 1.28 × 6 (18H, s, CH_3-12, CH_3-12′, CH_3-13, CH_3-13′, CH_3-14, and CH_3-14′). The ^{13}C NMR data (Table 1) of **1** showed 32 carbon resonances, including twelve aromatic carbons (δ_C 147.1 × 2, 146.9, 146.8, 138.5 × 2, 124.4 × 2, 124.1 × 2, and 119.0 × 2), four oxygenated carbons at (δ_C 69.7 × 4), four quaternary carbons (δ_C 34.5 × 2 and 34.3 × 2), and twelve methyl carbons (δ_C 31.2 × 2 and 30.1 × 2).

Comparison of NMR data of **1** and 2,2′-oxydiessigsaure-bis(2,4-di-tert-butylphenyl-ester) revealed that their differences were at C-15 and C-15′ (RuJhofer et al., 1979). In the HMBC spectrum, correlations of H-3 with C-5/C-7, H-3′ with C-5′/C-7′, H-6 with C-2/C-4, H-6′ with C-2′/C-4′, CH_3-10 with C-7/C-8/C-9, CH_3-10′ with C-7′/C-8′/C-9′, CH_3-12 with C-11/C-13/C-14, and CH_3-12′ with C-11′/C-13′/C-14′ revealed the presence of 2,4-di-tert-butylphenyl and 2′,4′-di-tert-butylphenyl moieties. In addition, HMBC correlations of H_2-15 with C-1/C-16, H_2-16 with C-16′, and H_2-15′ with C-1/C-16 suggested that the linkage of 2,4-di-tert-butylphenyl and 2′,4′-di-tert-butylphenyl moieties through an O–C-15–C-16–O–C-16′–C-15′–O moiety. The locations of four tert-butyl groups were further confirmed through a NOESY spectrum showing correlations of CH_3-10 with H-3, CH_3-12 with H-3/H-5, CH_3-10′ with H-3′, and CH_3-12′ with H-3′/H-5′. Accordingly, the structure of **1** was showed in Fig. 1, and it

ACCEPTED MANUSCRIPT

was named as uncariarhyine A.

In addition, the investigation of hooks of *U. rhynchophylla* led to the isolation of oleanic acid (**2**) (Yang et al., 2017), robustanic acid (**3**)(Khare et al., 2002), oleanderolide (**4**) (Fu et al., 2005), ursolic acid (**5**) (Liu et al., 2018), 3*β*,6*β*,19*α*-trihydroxy-urs-12-en-28-oic acid (**6**) (Calderon et al., 2009), 3*β*,6*β*-dihydroxy-urs-12-en-28-oic acid (**7**) (Wei et al., 2015), 3*β*,19*α*-dihydroxy-6-oxo-urs-12-en-28-oic acid (**8**) (Pradhan et al., 1987), *β*-amyrin (**9**) (Teng et al., 2000), dibutyl phthalate (**10**) (Ruikar et al., 2011), bluemenol A (**11**) (Yan et al., 2017), loliolide (**12**) (Peng et al., 2018), *trans*-cinnamic acid (**13**) (Teles et al., 2016), salicylic acid (**14**) (Li et al., 2015), terephthalic acid bis(2-ethyl-hexyl) ester (**15**) (Xu et al., 2015), noreugenin (**16**) (Okamura et al., 1998), (*S*)-5-hydroxy-3,4-dimethyl-5-pentylfuran-2(5*H*)-one (**17**) (Zhang et al., 2014), benzo[d]thiazol-2(3*H*)-one (**18**) (Fang et al., 2016), 3,3′,5,5′-tetra-*t*-butyl-2,2′-dihydroxydiphenyl (**19**) (Kaeding, 1963), ferulic acid (**20**) (Park et al., 2018), methyl caffeate (**21**) (Lima et al., 2018), ethyl caffeate (**22**) (Lee et al., 2016), and ethyl 3,4-dihydroxy benzoate (**23**) (Liu et al., 2015).

hCE 2 inhibitory effects.

Recently, some potent CEs inhibitors have been discovered, such as derivatives of tanshinones from the genus *Salvia* and lapachones from the genus *Handroanthus* (Binder et al., 2018; Hatfield et al., 2017), therefore, all the isolated compounds **1-23** and some ursane-type triterpenoids **24-29** were assayed for their inhibitory activities against hCE 2. Loperamide was used as a positive control had an IC_{50} value of 1.26 ±

ACCEPTED MANUSCRIPT

0.22 μM. Compounds **1-5**, **7**, **9**, and **15** displayed significant inhibitory activities against hCE 2 with IC_{50} values of 10.95 ± 0.52, 4.37 ± 0.29, 18.6 ± 0.21, 5.59 ± 0.25, 7.54 ± 0.24, 16.71 ± 0.89, 4.01 ± 0.61, and 15.40 ± 0.45 μM, respectively, whereas compounds **6**, **8**, and **10** showed moderate inhibitory activities with IC_{50} values of 40.90 ± 1.12, 51.78 ± 2.21, and 33.41 ± 1.52 μM, respectively.

Structure-activity relationship.

Some of triterpenoids including oleanane-type (**2**, **4**, and **9**) and ursane-type (**3**, **5-8**, and **23-29**) triterpenoids were assayed for their inhibitory activities against hCE 2. Therefore, structure-activity relationships of ursane-type triterpenoids were discussed (Fig. 3). Comparison of IC_{50} values of compounds **5** with **7** and **6** with **7** revealed that removal of C-6 and C-19 hydroxy groups was essential to inhibitory activity. Compound **3** had an IC_{50} value of 18.60 μM, whereas compound **5** displayed significant inhibitory activity with IC_{50} value of 7.54 μM, which indicated that C-11 methoxy substitution negatively affected its inhibitory activity. Oxidation of the hydroxy group at C-6 in compound **6** led to the production of compound **8**, and the latter displayed less inhibitory activity than the former, indicating that oxidation of C-6 hydroxy group was nonessential to inhibitory activity. Additionally, a comparison of inhibitory efficiency of compounds **5** and **24-29** revealed that increasing polarity of these triterpenoids is not beneficial to inhibitory activity.

Enzyme kinetics

Inhibition kinetics of compounds **1-5**, **7**, **9**, and **15** against hCE 2 were conducted by using Lineweaver-Burk plots to determine their inhibition type, and the results are

ACCEPTED MANUSCRIPT

listed in Fig. 4 and Table 3. As shown in Fig. 4, a series of lines of compounds **1-5**, **9**, and **15** intersected at a point in the negative X axis in the Lineweaver-Burk plots (Fig. 4), which indicated that inhibition type of compounds **1**, **5**, **9**, and **15** were noncompetitive type (Kim et al., 2018; Leem et al., 2017; Soares da Silva et al., 2018; Sohretoglu et al., 2018). Increasing concentration of compounds **3** and **4** resulted in the increase of Km and the decrease of Vmax, indicating that compounds **3** and **4** were mixed-type inhibitors (Kim et al., 2018; Leem et al., 2017; Soares da Silva et al., 2018; Sohretoglu et al., 2018), which were further confirmed by Lineweaver-Burk plots that showed a series of lines of compounds **3** and **4** crossing a point in the second quadrant (Fig. 4). In addition, a series of parallel lines of compounds **2** and **7** were shown in Fig. 4, and Km and Vmax decreased with increasing concentration of compounds **2** and **7**, suggesting that they were uncompetitive inhibitors (Kim et al., 2018; Leem et al., 2017; Soares da Silva et al., 2018; Sohretoglu et al., 2018).

Molecular docking

The interaction mode between compounds **1**-**5**, **7**, **9**, and **15** with hCE 2 was also investigated through molecular docking. As shown in Fig. 5 and 6, all the above-mentioned compounds could be docked into the catalytic site cavity of hCE 2. The hydroxy group at C-3 of compounds **2**, **3**, and **5** all formed hydrogen bonds with the catalytic site residue Gln81 of hCE 2, which indicated that they adopted similar binding mode. Compounds **2** and **5** formed additional hydrogen bonds with Glu225 and Ser200 respectively, which made their inhibitory activities better than compound **3**. For compound **4**, three hydrogen bonds were formed with the catalytic site residues

ACCEPTED MANUSCRIPT

Leu79, Gln81, and Glu199, respectively, which assured its strong inhibitory activity. The oxygen at C-16 of compound **1** formed hydrogen bonds with the catalytic site residue Gly430. The hydroxy group at C-3 and the carboxy group at C-28 of compound **7** formed two hydrogen bonds with the catalytic site residues Ser439 and Ala122, respectively, whereas the hydroxy group at C-3 of compound **9** interacted with Leu130 and Arg438. Correspondingly the carboxy group of compound **15** formed a hydrogen bond with Gln81.

Conclusions

In this study, the investigation of *Uncaria rhynchophylla* resulted in the isolation of one new compound **1** and twenty-two known compounds **2-23**. All the isolated compounds were evaluated for their inhibitory activities against hCE 2. Compounds **1**-**5**, **7**, **9**, and **15** showed significant inhibitory activities against hCE 2 with IC_{50} values from 4.01 ± 0.61 μM to 18.6 ± 0.21 μM, respectively. According to their inhibition kinetic results, compounds **1**, **5**, **9**, and **15** were non-competitive inhibitors with Ki values of 7.67, 8.64, 4.71, and 16.34 μM, respectively, compounds **3** and **4** were mixed-type inhibitors with Ki values of 25.63 and 9.14 μM, respectively, whereas compounds **2** and **7** were uncompetitive (Ki = 5.30 μM for **2**; Ki = 35.10 μM for **7**). The potential interaction mechanisms of compounds **1**-**5**, **7**, **9**, and **15** with hCE 2 were also analysed by molecular docking.

Conflict of interest

The authors declare no competing financial interest.

Acknowledgments

This work was supported by National Natural Science Foundation of China (No. 81703679 and 81622047), Distinguished professor of Liaoning Province, and Natural

ACCEPTED MANUSCRIPT

Science Foundation of Institute of Integrative Medicine, Dalian Medical University (ICIM2017001).

References

Ai, C.Z., Li, Y., Wang, Y.H., Li, W., Dong, P.P., Ge, G.B., Yang, L., 2010. Investigation of binding features: effects on the interaction between CYP2A6 and inhibitors. J. Comput. Chem. 31, 1822-1831.

Bencharit, S., Edwards, C.C., Morton, C.L., Howard-Williams, E.L., Kuhn, P., Potter, P.M., Redinbo, M.R., 2006. Multisite promiscuity in the processing of endogenous substrates by human carboxylesterase 1. J. Mol. Biol. 363, 201-214.

Binder, R.J., Hatfield, M.J., Chi, L.Y., Potter, P.M., 2018. Facile synthesis of 1,2-dione-containing abietane analogues for the generation of human carboxylesterase inhibitors. Eur. J. Med. Chem. 149, 79-89.

Calderon, A.I., Simithy, J., Quaggio, G., Espinosa, A., Lopez-Perez, J.L., Gupta, M.P., 2009. Triterpenes from *Warszewiczia coccinea* (Rubiaceae) as inhibitors of acetylcholinesterase. Nat. Prod. Commun. 4, 1323-1326.

Cang, J., Wang, C., Huo, X.K., Tian, X.G., Sun, C.P., Deng, S., Zhang, B.J., Zhang, H.L., Liu, K.X., Ma, X.C., 2017. Sesquiterpenes and triterpenoids from the rhizomes of *Alisma orientalis* and their pancreatic lipase inhibitory activities. Phytochem. Lett. 19, 83-88.

Fang, S.S., Tang, C., Ye, K.Y., Lu, X.L., Liu, X.Y., Jiao, B.H., 2016. Studies on the secondary metabolites from antarctic-derived fungus *Penicillium* sp. S-3-88. Chinese Journal of Marine Drugs 35, 28-30.

ACCEPTED MANUSCRIPT

Fu, L.W., Zhang, S.J., Li, N., Wang, J.L., Zhao, M., Sakai, J., Hasegawa, T., Mitsui, T., Kataoka, T., Oka, S., Kiuchi, M., Hirose, K., Ando, M., 2005. Three new triterpenes from *Nerium oleander* and biological activity of the isolated compounds. J. Nat. Prod. 68, 198-206.

Geng, C.A., Huang, X.Y., Ma, Y.B., Hou, B., Li, T.Z., Zhang, X.M., Chen, J.J., 2017. (+/-)-Uncarilins A and B, Dimeric isoechinulin-type alkaloids from *Uncaria rhynchophylla*. J. Nat. Prod. 80, 959-964.

Hatfield, M.J., Chen, J.W., Fratt, E.M., Chi, L.Y., Bollinger, J.C., Binder, R.J., Bowling, J., Hyatt, J.L., Scarborough, J., Jeffries, C., Potter, P.M., 2017. Selective inhibitors of human liver carboxylesterase based on a beta-lapachone scaffold: Novel reagents for reaction profiling. J. Med. Chem. 60, 1568-1579.

Huo, X.K., Liu, J., Yu, Z.L., Wang, Y.F., Wang, C., Tian, X.G., Ning, J., Feng, L., Sun, C.P., Zhang, B.J., Ma, X.C., 2018. *Alisma orientale* extract exerts the reversing cholestasis effect by activation of farnesoid X receptor. Phytomedicine 42, 34-42.

Kaeding, W.W., 1963. Oxidation of phenols with cupric salts J. Org. Chem. 28, 1063-1067.

Khare, M., Srivastava, S.K., Singh, A.K., 2002. A new triterpenic acid from *Eucalyptus robusta*. Indian J. Chem. B 41, 440-445.

Kim, J.H., Cho, I.S., Ryu, J., Lee, J.S., Kang, J.S., Kang, S.Y., Kim, Y.H., 2018. *In vitro* and in silico investigation of anthocyanin derivatives as soluble epoxide hydrolase inhibitors. Int. J. Biol. Macromol. 112, 961-967.

Lee, S.J., Jang, H.J., Kim, Y., Oh, H.M., Lee, S., Jung, K., Kim, Y.H., Lee, W.S., Lee,

S.W., Rho, M.C., 2016. Inhibitory effects of IL-6-induced STAT3 activation of bio-active compounds derived from *Salvia plebeia* R.Br. Process Biochem. 51, 2222-2229.

Leem, H.H., Lee, G.Y., Lee, J.S., Lee, H., Kim, J.H., Kim, Y.H., 2017. Soluble epoxide hydrolase inhibitory activity of components from *Leonurus japonicus*. Int. J. Biol. Macromol. 103, 451-457.

Li, J., Chaytor, J.L., Findlay, B., McMullen, L.M., Smith, D.C., Vederas, J.C., 2015. Identification of didecyldimethylammonium salts and salicylic acid as antimicrobial compounds in commercial fermented radish kimchi. J. Agric. Food Chem. 63, 3053-3058.

Li, R.X., Cheng, J.T., Jiao, M.J., Li, L., Guo, C., Chen, S., Liu, A., 2017. New phenylpropanoid-substituted flavan-3-ols and flavonols from the leaves of *Uncaria rhynchophylla*. Fitoterapia 116, 17-23.

Lima, T.C., Ferreira, A.R., Silva, D.F., Lima, E.O., de Sousa, D.P., 2018. Antifungal activity of cinnamic acid and benzoic acid esters against *Candida albicans* strains. Nat. Prod. Res. 32, 572-575.

Liu, X., Yin, C.L., Cao, Y., Zhou, J.G., Wu, T., Cheng, Z.H., 2018. Chemical constituents from *Gueldenstaedtia verna* and their anti-inflammatory activity. Nat. Prod. Res. 32, 1145-1149.

Liu, X.F., Ding, M.L., Zhang, C.F., Zhang, M., Xu, X.H., 2015. Nor-C21 steroidal constituents from the roots of *Cynanchum ascyrifolium*. Pharmaceutical and Clinical Research 23, 123-126.

ACCEPTED MANUSCRIPT

Ndagijimana, A., Wang, X.M., Pan, G.X., Zhang, F., Feng, H., Olaleye, O., 2013. A review on indole alkaloids isolated from *Uncaria rhynchophylla* and their pharmacological studies. Fitoterapia 86, 35-47.

Okamura, N., Hine, N., Tateyama, Y., Nakazawa, M., Fujioka, T., Mihashi, K., Yagi, A., 1998. Five chromones from *Aloe vera* leaves. Phytochemistry 49, 219-223.

Park, H.J., Cho, J.H., Hong, S.H., Kim, D.H., Jung, H.Y., Kang, I.K., Cho, Y.J., 2018. Whitening and anti-wrinkle activities of ferulic acid isolated from *Tetragonia tetragonioides* in B16F10 melanoma and CCD-986sk fibroblast cells. J. Nat. Med. 72, 127-135.

Peng, Y., Huang, R.M., Lin, X.P., Liu, Y.H., 2018. Norisoprenoids from the Brown alga Sargassum naozhouense Tseng et Lu. Molecules 23, 348.

Potter, P.M., Wadkins, R.M., 2006. Carboxylesterases--detoxifying enzymes and targets for drug therapy. Curr. Med. Chem. 13, 1045-1054.

Pradhan, B.P., Chakraborty, S., Weyerstahl, P., 1987. Studies on oxidation of triterpenoids. Part VII. Transformation of oleanane and ursane skeletons to 11a,12a-oxidotriterpenoids with hydrogen peroxide and selenium dioxide and their carbon-13 NMR data. Tetrahedron 43, 4487-4495.

Ross, M.K., Crow, J.A., 2007. Human carboxylesterases and their role in xenobiotic and endobiotic metabolism. J. Biochem. Mol. Toxicol. 21, 187-196.

Ruikar, A.D., Gadkari, T.V., Phalgune, U.D., Puranik, V.G., Deshpande, N.R., 2011. Dibutyl phthalate, a secondary metabolite from *Mimusops elengi*. Chem. Nat. Compd. 46, 955-956.

ACCEPTED MANUSCRIPT

RuJhofer, W., Miiller, W.M., Vogtle, F., 1979. Nichtcyclische kronenether-artige ester und ihre metallion-komplexe. Chem. Ber. 112, 2095-2119.

Satoh, T., Hosokawa, M., 1998. The mammalian carboxylesterases: from molecules to functions. Annu. Rev. Pharmacol. Toxicol. 38, 257-288.

Soares da Silva, O., Lira de Oliveira, R., de Carvalho Silva, J., Converti, A., Souza Porto, T., 2018. Thermodynamic investigation of an alkaline protease from *Aspergillus tamarii* URM4634: A comparative approach between crude extract and purified enzyme. Int. J. Biol. Macromol. 109, 1039-1044.

Sohretoglu, D., Sari, S., Soral, M., Barut, B., Ozel, A., Liptaj, T., 2018. Potential of *Potentilla inclinata* and its polyphenolic compounds in alpha-glucosidase inhibition: Kinetics and interaction mechanism merged with docking simulations. Int. J. Biol. Macromol. 108, 81-87.

Teles, Y.C.F., Ribeiro, J., Bozza, P.T., Agra, M.D., Siheri, W., Igoli, J.O., Gray, A.I., de Souza, M.D.V., 2016. Phenolic constituents from *Wissadula periplocifolia* (L.) C. Presl. and anti-inflammatory activity of 7,4'-di-*O*-methylisoscutellarein. Nat. Prod. Res. 30, 1880-1884.

Teng, R.W., Wang, D.Z., Yang, C.R., 2000. Chemical constituents from *Balanopora harlandii*. Acta Botanica Yunnanica 22, 225-233.

Wang, C., Huo, X.K., Luan, Z.L., Cao, F., Tian, X.G., Zhao, X.Y., Sun, C.P., Feng, L., Ning, J., Zhang, B.J., Ma, X.C., 2017. Alismanin A, a triterpenoid with a C_{34} skeleton from *Alisma orientale* as a natural agonist of human pregnane X receptor. Org. Lett. 19, 5645-5648.

ACCEPTED MANUSCRIPT

Wei, Y.D., Yan, L.H., Liang, H., Zhu, M.Z., Ye, D.L., Zhang, Q.Y., 2015. Triterpenoids from the stems of *Uncaria macrophylla*. Journal of Chinese Pharmaceutical Sciences 24, 292−302

Wheelock, C.E., Phillips, B.M., Anderson, B.S., Miller, J.L., Miller, M.J., Hammock, B.D., 2008. Applications of carboxylesterase activity in environmental monitoring and toxicity identification evaluations (TIEs). Rev. Environ. Contam. Toxicol. 195, 117-178.

Xin, X.L., Zhao, X.Y., Huo, X.K., Tian, X.G., Sun, C.P., Zhang, H.L., Tian, Y., Liu, Y., Wang, X., 2018. Two new protostane-type triterpenoids from *Alisma orientalis*. Nat. Prod. Res. 32, 189-194.

Xu, Y., Tian, S.S., Zhu, H.J., 2015. A new lactone aldehyde compound isolated from secondary metabolites of marine fungus *Penicillium griseofulvum*. Natural Product Research and Development 27, 559-561.

Yan, X.J., Zheng, W., Wen, J., Wu, J., Xu, Y., Cao, L., Wang, H.X., Xiang, Z., 2017. Chemical constituents of *Patrinia villosa*. Chinese Traditional and Herbal Drugs 48, 247-251.

Yang, L.Y., Lin, J., Zhou, B., Liu, Y.G., Zhu, B.Q., 2017. Activity of compounds from Taxillus sutchuenensis as inhibitors of HCV NS3 serine protease. Nat. Prod. Res. 31, 487-491.

Yu, Z.L., Peng, Y.L., Wang, C., Cao, F., Huo, X.K., Tian, X.G., Feng, L., Ning, J., Zhang, B.J., Sun, C.P., Ma, X.C., 2017. Alismanoid A, an unprecedented 1,2-*seco* bisabolene from *Alisma orientale*, and its protective activity against H_2O_2-induced

damage in SH-SY5Y cells. New J. Chem. 41, 12664-12670.

Zhang, J., Liang, Y., Liao, X.J., Deng, Z., Xu, S.H., 2014. Isolation of a new butenolide from the South China Sea gorgonian coral *Subergorgia suberosa*. Nat. Prod. Res. 28, 150-155.

Zhang, Q., Zhao, J.J., Xu, J., Feng, F., Qu, W., 2015. Medicinal uses, phytochemistry and pharmacology of the genus *Uncaria*. J. Ethnopharmacol. 173, 48-80.

Zhang, Z.J., Huo, X.K., Tian, X.G., Feng, L., Ning, J., Zhao, X.Y., Sun, C.P., Wang, C., Deng, S., Zhang, B.J., Zhang, H.L., Liu, Y., 2017. Novel protostane-type triterpenoids with inhibitory human carboxylesterase 2 activities. Rsc Adv. 7, 28702-28710.

Zou, L.W., Li, Y.G., Wang, P., Zhou, K., Hou, J., Jin, Q., Hao, D.C., Ge, G.B., Yang, L., 2016. Design, synthesis, and structure-activity relationship study of glycyrrhetinic acid derivatives as potent and selective inhibitors against human carboxylesterase 2. Eur. J. Med. Chem. 112, 280-288.

ACCEPTED MANUSCRIPT

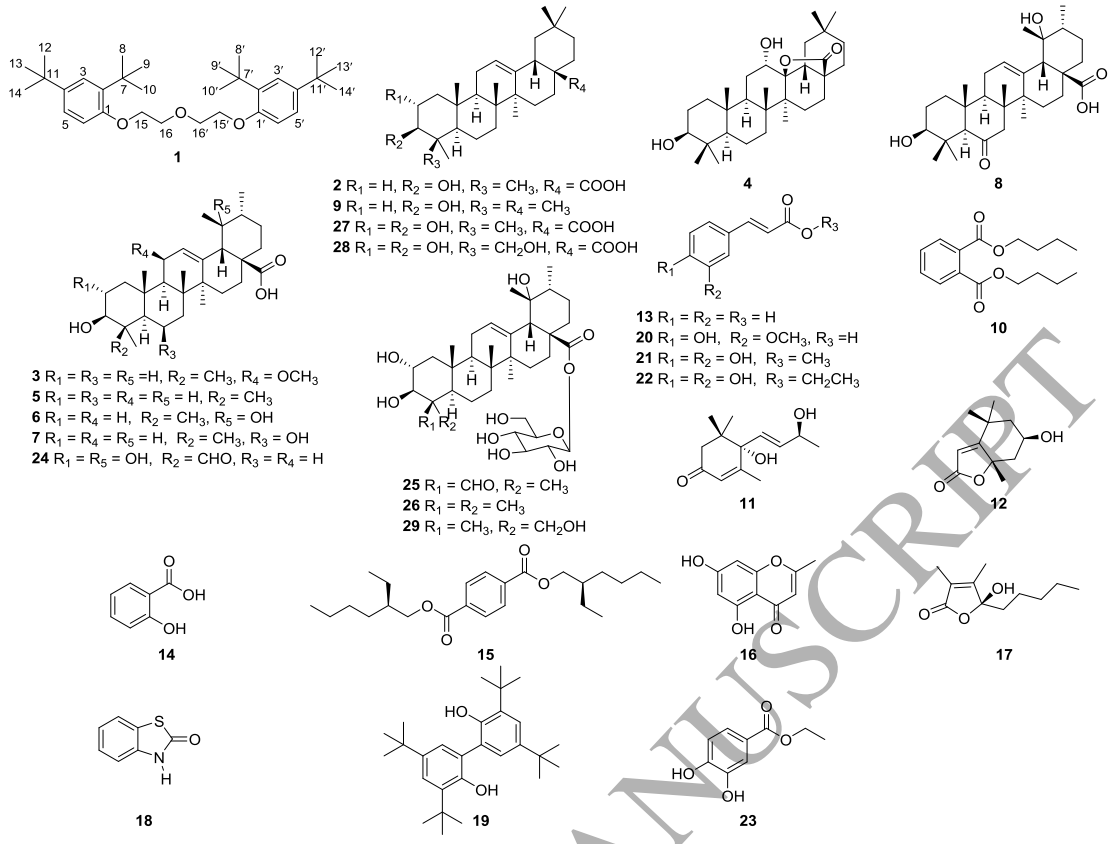

Fig. 1. Structure of compounds **1-29**

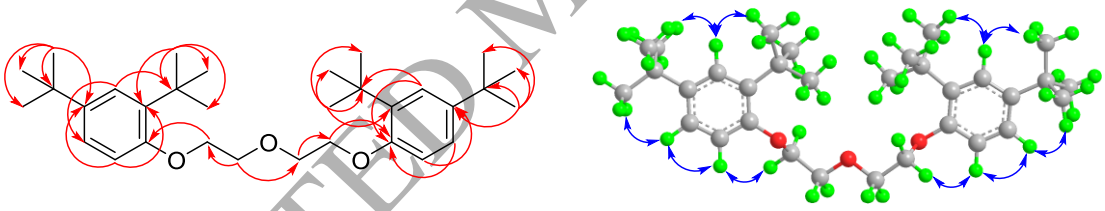

Fig. 2. Selected HMBC and NOESY correlations of compound **1**

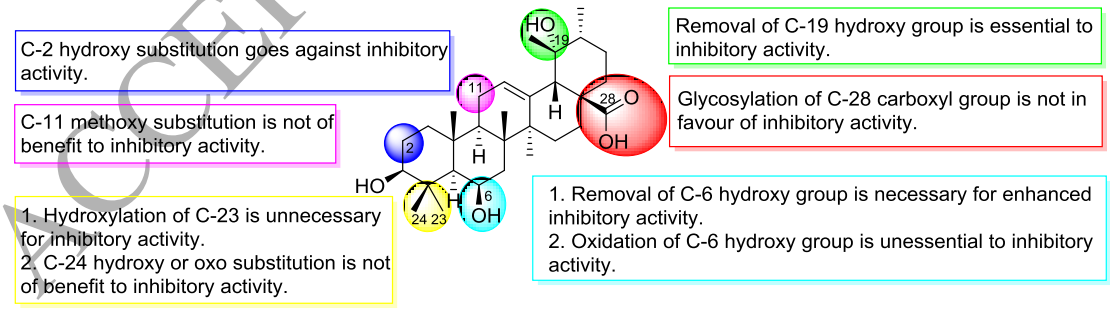

Fig. 3. Structure-activity relationship of ursane-type triterpenoids

ACCEPTED MANUSCRIPT

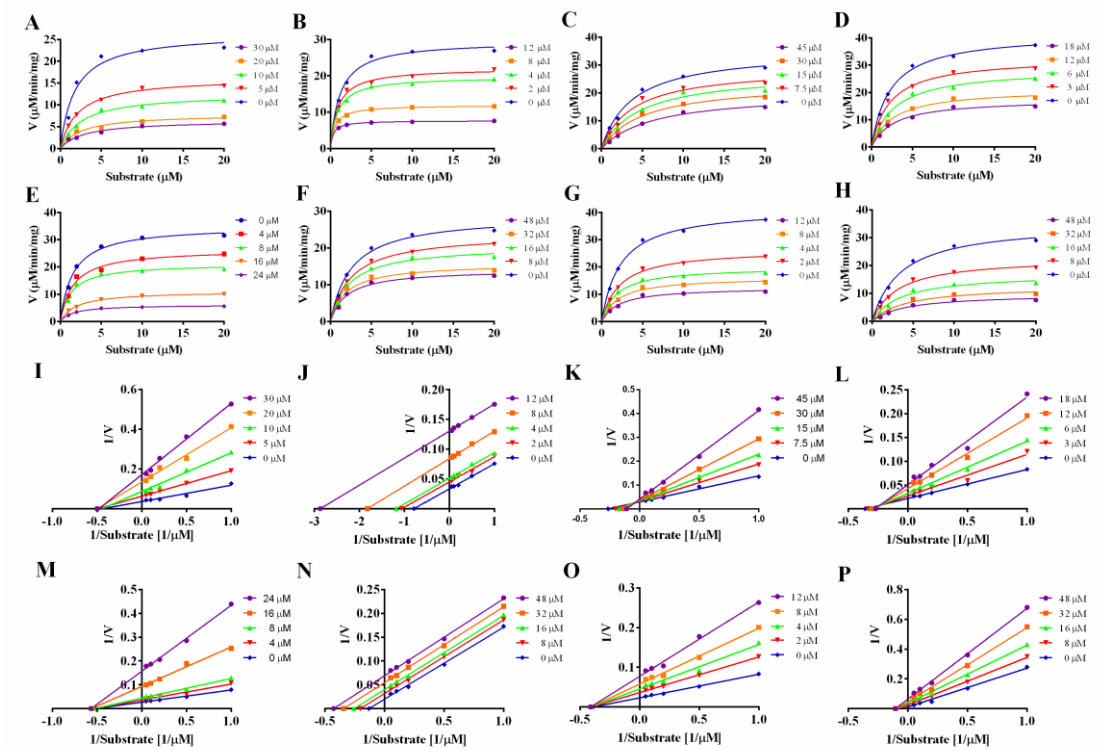

Fig. 4. Inhibitory kinetics and Lineweaver-Burk plots of compounds **1-5** (A-E and I-M), **7** (F and N), **9** (G and O), and **15** (H and P) against hCE 2.

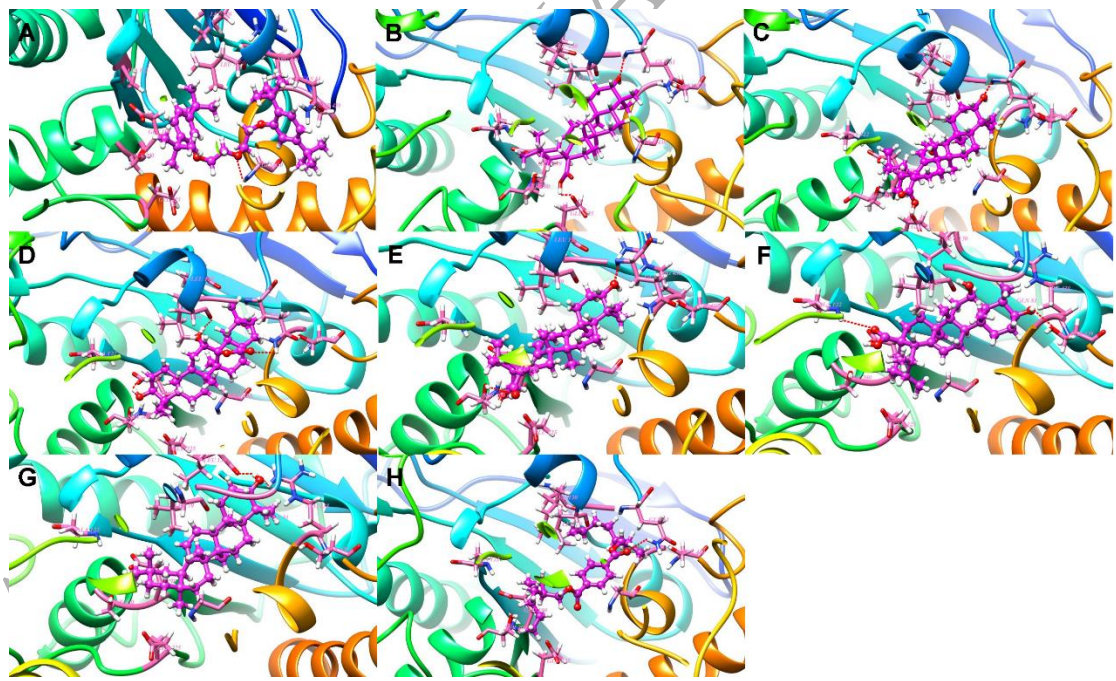

Fig. 5. 3D structures of compounds **1-5** (A-E), **7** (F), **9** (G), and **15** (H) with hCE 2 (red dotted line, hydrogen bond interaction)

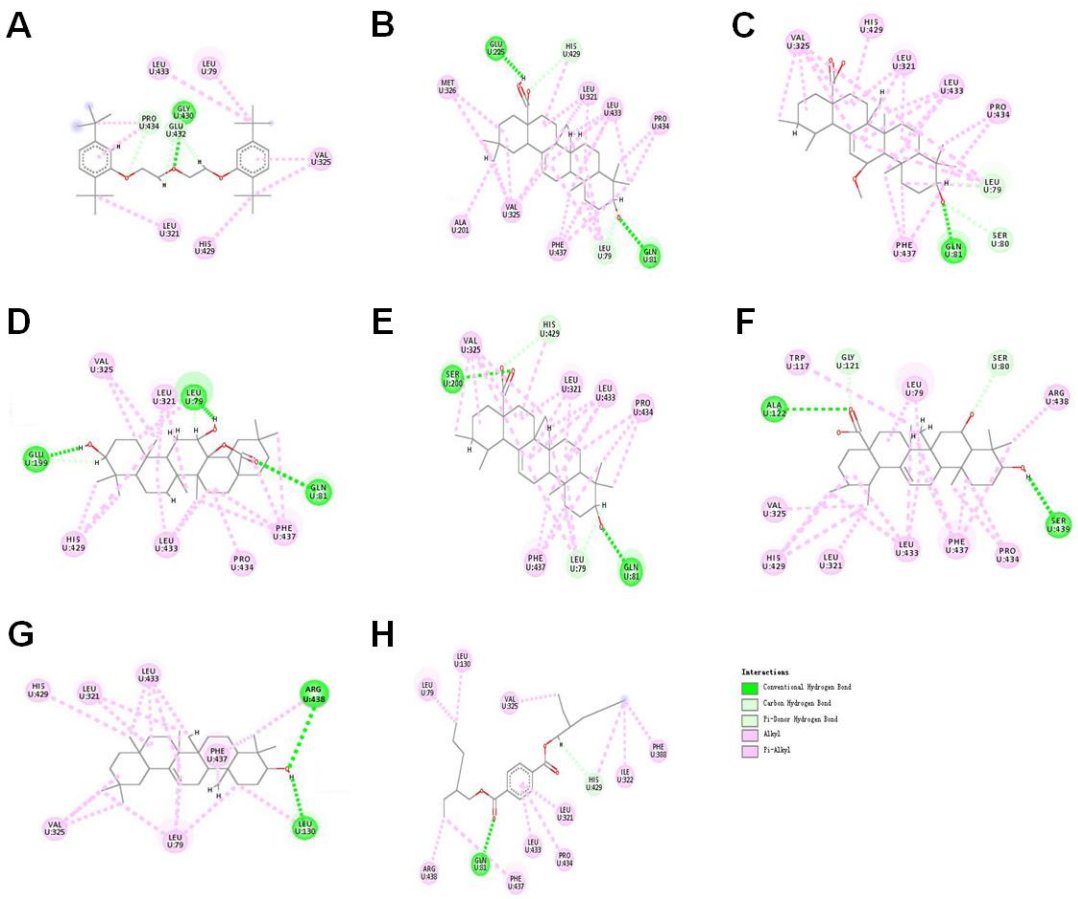

Fig. 6. Interactions of compounds **1**-**5** (A-E), **7** (F), **9** (G), and **15** (H) with hCE 2

Table 1. ^{1}H (600 MHz) and ^{13}C NMR (150 MHz) data of compound **1** in DMSO-d_6

No.	δ_C	δ_H (J in Hz)	No.	δ_C	δ_H (J in Hz)

1	146.8		1′	146.9	
2	138.5		2′	138.5	
3	124.1	7.37 d (2.4)	3′	124.1	7.37 d (2.4)
4	147.1		4′	147.1	
5	124.4	7.29 dd (8.5, 2.4)	5′	124.4	7.29 dd (8.5, 2.4)
6	119.0		6′	119.0	
7	34.5		7′	34.5	
8	30.1	1.39 s	8′	30.1	1.39 s
9	30.1	1.39 s	9′	30.1	1.39 s
10	30.1	1.39 s	10	30.1	1.39 s
11	34.3		11′	34.3	
12	31.2	1.28 s	12′	31.2	1.28 s
13	31.2	1.28 s	13′	31.2	1.28 s
14	31.2	1.28 s	14′	31.2	1.28 s
15	69.7	4.79 t (11.5)	15′	69.7	4.82 t (11.5)
16	69.7	4.48 t (11.5)	16′	69.7	4.52 t (11.5)

Table 2. Inhibitory effects of compounds **1-29** against hCE 2.

Compounds	Inhibition of compounds against hCE 2	
	100 μM (%)	IC_{50} values (μM)
1	90.96 ± 1.56	10.95 ± 0.52
2	90.96 ± 1.49	4.37 ± 0.29
3	87.06 ± 1.23	18.60 ± 0.21
4	92.08 ± 2.15	5.59 ±0.25
5	98.44 ± 1.46	7.54 ± 0.24
6	74.45 ± 2.01	40.90 ± 1.12
7	86.06 ± 1.25	16.71 ± 0.89
8	74.36 ± 1.21	51.78 ± 2.21
9	87.83 ± 1.32	4.01 ± 0.61
10	68.85 ± 2.32	33.41 ± 1.52
11	27.30 ± 0.89	> 100
12	44.86 ± 0.54	> 100
13	56.31 ± 1.32	96.43 ± 2.41
14	56.22 ± 1.35	82.31 ± 1.62
15	92.27 ± 1.03	15.40 ± 0.45
16	58.91 ± 1.78	90.21 ± 1.23
17	61.68 ± 2.01	75.21 ± 1.45
18	29.79 ± 1.25	> 100
19	82.61 ± 3.25	72.30 ± 1.82

ACCEPTED MANUSCRIPT

20	21.01 ± 0.23	> 100
21	8.47 ± 0.11	> 100
22	9.12 ± 0.54	> 100
23	27.15 ± 1.28	> 100
24	39.33 ± 2.35	> 100
25	19.64 ± 0.85	> 100
26	26.12± 1.64	> 100
27	59.95 ± .45	85.43 ± 1.23
28	15.32 ± 1.32	> 100
29	13.61 ± 1.55	> 100
Loperamide[a]	99.87 ± 0.11	1.26 ± 0.12

[a]Loperamide as a positive control.

Table 3. Kinetic parameters of compounds **1**-**5**, **7**, **9**, and **15** against hCE 2.

Compounds	Inhibition type	Vmax (μM/min/mg)	Km (μM)	Ki (μM)
1	Noncompetitive	26.92	1.98	7.67
2	Uncompetitive	30.33	1.24	5.30
3	Mixed	34.42	3.67	25.63
4	Mixed	41.34	2.25	9.13
5	Noncompetitive	36.07	1.54	8.64
7	Uncompetitive	29.81	3.10	35.10
9	Noncompetitive	40.24	2.16	4.71
15	Noncompetitive	35.04	3.48	16.34

Table 4. Interaction information of compounds **1**-**5**, **7**, **9**, and **15** with hCE 2.

Compounds	Interaction amino acids	Hydrogen bonds	Chemscore (kcal/mol)
1	Leu79, Val325, His429, Gly430, Glu432, Leu433, Pro434	Gly430	-54.038
2	Leu79, Gln81, Ala201, Glu225, Leu321, Met326, Val325, His429, Leu433, Pro434, Phe437	Gln81, Glu225	-52.144
3	Leu79, Ser80, Gln81, Leu321, Val325, His429, Leu433, Pro434, Phe437	Gln81	-50.779
4	Leu79, Gln81, Gln199, Leu321, Val325, His429,	Leu79, Gln81, Glu199	-51.219

	Leu433, Pro434, Phe437		
5	Leu79, Gln81, Ser200, Leu321, Val325, His429, Leu433, Pro434, Phe437	Gln81, Ser200	-53.343
7	Leu79, Ser80, Trp117, Gly121, Ala122, Leu321 Val325, His429, Leu433, Pro434, Phe437, Arg438, Ser439	Ala122, Ser439	-49.785
9	Leu79, Leu130, Leu321, Val325, His429, Leu433, Phe437, Arg438	Leu130, Arg438	-55.995
15	Leu79, Gln81, Leu130, Leu321, Ile322, Val325, Phe388, His429, Leu433, Pro434, Phe437, Arg438	Gln81	-40.995

ACCEPTED MANUSCRIPT

Graphical Abstract

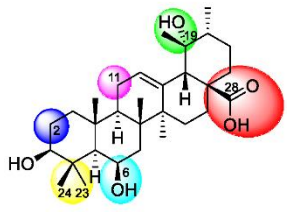

Structure-activity relationship

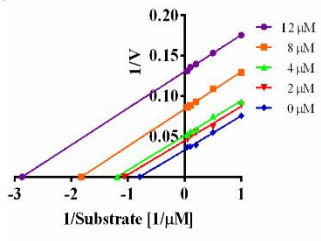

Lineweaver-Burk plot

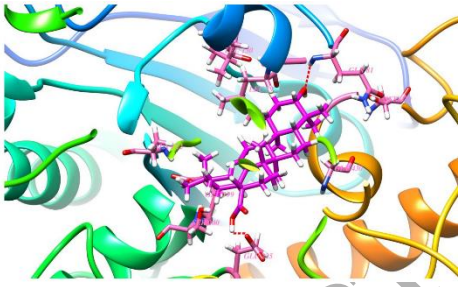

ACCEPTED MANUSCRIPT